A theoretical study on the ionization of pyrrole with analysis of vibrational structure of the photoelectron spectra

Kouichi Takeshita
Faculty of Bioindustry, Tokyo University of Agriculture, Abashiri, Hokkaido 099-24, Japan

Yuichi Yamamoto
The Center for Information Processing Education of Hokkaido University, Sapporo 060 Japan

(Received 4 March 1994; accepted 20 April 1994)

Ab initio calculations have been performed to study on the molecular structures and the vibrational levels of the low-lying ionic states ($^2A_2$, $^2B_1$, $^2A_1$, and $^2B_2$) of pyrrole. The equilibrium molecular structures and vibrational modes of these states are presented. The theoretical ionization intensity curves including the vibrational structure of the low-lying two ionic states are also presented and compared with the photoelectron spectrum. A number of new assignments of the photoelectron spectra are proposed.

I. INTRODUCTION

The electronic configuration of the ground state of pyrrole is represented by a $\cdots(8a_1)^2(5b_2)^2(1b_1)^2(4b_2)^2(9a_1)^2(2b_1)^2(1a_2)^2$.

The photoelectron (PE) spectroscopy investigations of pyrrole have reported by many workers.[1-7] The assignment of the electronic states of the lowest two bands were established. The lowest state was the $^2A_2$ state and the second was the $^2B_1$ state. These states show well resolved vibrational structure. The assignment of the vibrational levels was attempted by Derrick *et al.*[3] They interpreted the vibrational structure by taking account of the vibrational frequencies of the ground state. The third band of the 12–16 eV region contains several electronic states.

The theoretical approaches on pyrrole have been reported.[8-11] Many workers have calculated the vertical ionization energies in order to help the assignment of the electronic states of the PE spectra. The vertical ionization energy was calculated by the use of the geometry in the ground state.

As a molecule is ionized, the equilibrium molecular structure and the character of the vibrational mode should change from those of the ground state. The vibrational structure of the PE spectrum reflects these changes. It is therefore interesting to investigate the vibrational structure associated with the change in the equilibrium molecular structure and the vibrational mode by ionization.

Any theoretical investigation on the molecular structures and the vibrational levels of the ionic states has not been reported. In this work, we determine the equilibrium molecular structures of the ground and lowest ionic states by using the *ab initio* self-consistent-field (SCF) method. Within the framework of the adiabatic approximation and the harmonic oscillator approximation, we calculated the harmonic force constant matrix elements over variables of the totally symmetric distortion and the vibrational frequencies of the totally symmetric modes. We obtained approximate theoretical intensity curves using the Franck–Condon factor (FCF) which was given by the square of the overlap integrals between the vibrational wave function of the ground state and that of the ionic state. Based on these calculations, we discuss the vibrational levels of the low-lying ionic states compared to the photoelectron spectrum.

II. METHOD OF CALCULATIONS

We used the basis sets of the MIDI-4-type prepared by Tatewaki and Huzinaga.[12] These were augmented by one p-type polarization function for H and one d-type polarization function for C and N. The exponents of the polarization function for H, C, and N were 0.68, 0.61, and 0.87, respectively.

The gradient technique for the Roothaan's restricted Hartree–Fock (RHF) method was employed to determine the optimum molecular structures of the ground state and the ionic states.

The single and double excitation configuration interaction (SDCI) method was employed to obtain more accurate ionization energies for the estimation of vertical ionization energy (VIE) and adiabatic ionization energy (AIE). A single reference configuration of an SCF wave function of the respective state was employed. In the SDCI method, singly and doubly excited configuration state functions (CSFs) were generated where the inner shells were kept frozen. The generated CSFs were then restricted to the first order interacting space.[13] The dimensions of the CI were too large, we adopted a CSF selection process by the use of second-order perturbation theory. The threshold for the selection was 8 μhartree. The number of the generated CSFs were reduced from about 135 000 to 15 500. We estimated the total energy including the contribution from the rejected CSFs by second-order perturbation theory.[14] The harmonic force constant matrix elements were calculated by means of the gradient technique with an RHF wave function; the second derivative was estimated by the numerical differentiation of the analytically calculated first derivative. We calculated the FCFs of only the totally symmetric vibrational modes. In calculating FCFs, we approximated the vibrational wave functions by those obtained by the harmonic oscillator model. We assumed that the initial state was the zero point vibrational level of the ground state. The method of calculation of the FCF and theoretical intensity curves was the same as we used in the previous paper.[15]

 0021-9606/94/101(3)/2198/7/$6.00

TABLE I. Optimized molecular structure and magnitude of the change in the geometry by ionization.

State	$N-C_2(\Delta N-C_2)$	$C_2-C_3(\Delta C_2-C_3)$	$C_2-H(\Delta C_2-H)$	$C_3-H(\Delta C_3-H)$	$N-H(\Delta N-H)$
$^1A_1$	1.362	1.362	1.078	1.079	0.996
Exp.[a]	1.370	1.382	1.076	1.077	0.996
$^2A_2$	1.345(−0.017)	1.424(+0.062)	1.080(+0.002)	1.078(−0.001)	1.004(+0.008)
$^2B_1$	1.355(−0.007)	1.363(+0.001)	1.077(−0.001)	1.079(+0.0)	1.009(+0.013)
$^2A_1$	1.352(−0.010)	1.329(−0.033)	1.083(+0.005)	1.078(−0.001)	1.001(+0.005)
$^2B_2$	1.340(−0.022)	1.431(+0.069)	1.078(+0.0)	1.120(+0.041)	1.005(+0.009)

State	$C_2-N-C_5(\Delta C_2-N-C_5)$	$N-C_2-C_3(\Delta N-C_2-C_3)$	$N-C_2-H(\Delta N-C_2-H)$	$C_2-C_3-H(\Delta C_2-C_3-H)$
$^1A_1$	109.58	108.17	121.22	125.92
Exp.[a]	109.8	107.7	121.5	125.5
$^2A_2$	109.16(−0.42)	108.48(+0.31)	121.88(+0.66)	124.81(−1.11)
$^2B_1$	113.96(+4.38)	106.54(−1.63)	122.04(+0.82)	127.43(+1.51)
$^2A_1$	111.29(+1.71)	114.30(+6.13)	122.82(+1.60)	149.68(+23.76)
$^2B_2$	110.78(+1.20)	106.74(−1.43)	127.76(+6.54)	111.88(−14.04)

[a]Nygaard *et al.* (Ref. 17). Bond lengths are in angstroms, angles in degrees. The values in parenthesis are the magnitude of the change in geometrical parameters by ionization.

This work was carried out by using the computer program system GRAMOL[16] for the gradient technique and the calculation of normal modes, and MICA3[17] for the CI calculations.

III. RESULTS AND DISCUSSION

The results of the optimized geometrical parameters of the ground and ionic states are listed in Table I. A numbering of each atom is illustrated in Fig. 1. The optimized geometric parameters of the ground state was in good agreement with the experimental ones.[18] Table I also shows a magnitude of the change in the equilibrium molecular structure by ionization.

Table II shows the VIE and AIE at the SCF and SDCI levels. In the SDCI calculations, the weight of the reference function of the $^1A_1$, $^2A_2$, $^2B_1$, $^2A_1$, and $^2B_2$ states at the optimized geometry were 86.2%, 86.4%, 86.0%, 86.0%, and 85.4%, respectively. Table II shows the energy lowering of the AIE compared with the VIE. We notice that the energy lowering of the $^2A_2$ and $^2B_1$ states at the SDCI level are smaller than 0.3 eV. While, those of the $^2A_1$ and $^2B_2$ states are larger than 1 eV.

The 0–0 ionization energies and the FCFs of the 0–0 transitions are listed in Table III. Derrick *et al.*[3] reported that the observed 0–0 bands of the the $^2A_2$ and $^2B_1$ states were 8.2 and 9.2 eV, respectively. The present calculated values are underestimated by 0.66 eV in comparison with the observed values. The FCFs of the $^2A_2$ and $^2B_1$ states are so large as to be able to be observed the 0–0 transition. The zero-point vibrational level of the $^2A_1$ state should not be observed, because the FCF is negligibly small.

The vibrational frequencies of the ground and ionic states are show in Table IV. The frequencies are arranged in order of magnitude. Comparing with the observed values[19] of $^1A_1$, we overestimate the frequencies by 9.4%–15.1% for the $\nu_1-\nu_5$ modes. The frequencies of the $\nu_6-\nu_7$ modes are overestimate by 1.0%–1.8%. An error of the ν_9 mode is 26%. However, Derrick *et al.* reported the frequency of 865 cm^{-1} of the ν_9 mode. Comparing with this value, we overestimate by 11.1%. Each mode is characterized by the use of the conventional potential energy distribution (PED) and the classical half amplitude of the zero-point vibrational levels. Table V shows the PED which is described using the totally symmetrical displacement coordinate.

For the interpretation of each mode of the $^1A_1$ state, Table V reveals that the PED of the ν_1 mode have a large

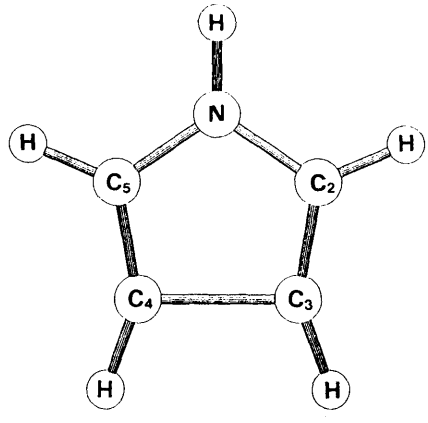

FIG. 1. A numbering of each atom.

TABLE II. Ionization energies (eV). VIE: Vertical ionization energy. AIE: Adiabatic ionization energy. Total energies (a.u.) of $^1A_1$: −208.579 316(SCF) and −209.197 273(SDCI).

	VIE		AIE		Δ(VIE–AIE)	
State	SCF	SDCI	SCF	SDCI	SCF	SDCI
$^2A_2$	7.17	7.82	6.90	7.53	0.27	0.29
$^2B_1$	8.29	8.74	8.14	8.57	0.15	0.17
$^2A_1$	12.45	12.76	11.00	11.64	1.44	1.12
$^2B_2$	13.80	14.47	13.14	12.95	0.66	1.52

TABLE III. 0–0 ionization levels. 0–0 IE: 0–0 ionization energy. FCF: Franck–Condon factor.

State	0–0 IE	FCF
$^2A_2$	7.54	0.211
$^2B_1$	8.54	0.330
$^2A_1$	11.59	0.000
$^2B_2$	12.88	0.022

value in the ΔS_5 totally symmetrical displacement coordinate which is connected to the N–H stretching motion. Therefore, we should assign obviously that the ν_1 mode is the N–H stretching mode. The ΔS_3 and ΔS_4 coordinates contribute to the PED of the ν_2 and ν_3 modes. The totally symmetrical displacement coordinates of the ΔS_3 and ΔS_4 are connected to the C_2–H (and C_5–H) stretching and C_3–H (and C_4–H) stretching motions, respectively. Thus the ν_2 and ν_3 modes are mixture of the C_2–H stretching and C_3–H stretching motions. The main component of the ν_2 and ν_3 modes are the C_2–H stretching and C_3–H stretching motions, respectively. Table VI reveals that the C_2–H stretching and C_3–H stretching motions mixes in phase for the ν_2 mode and out of phase for the ν_3 mode. The ν_9 mode is a mixture of the ΔS_6 and ΔS_7 coordinates. The totally symmetrical displacement coordinates of the ΔS_6 and ΔS_7 are the C–N–C bending and N–C–C bending motions, respectively. Table VI shows that the two motions couple out of phase. We are not able to make clear-cut interpretations of the ν_4, ν_5, ν_6, ν_7, and ν_8 modes. The ΔS_1, ΔS_3, ΔS_6, ΔS_7, ΔS_8, and ΔS_9 coordinates contribute to these modes, while the contributions of the ΔS_3, ΔS_4, and ΔS_5 coordinates are negligibly small.

The character of the ν_1 mode of the $^2A_2$, $^2B_1$, $^2A_1$, and $^2B_2$ states is the same as that of the ground state. It is assigned to the N–H stretching motion. It is indicated from Tables V and VI that the ν_2 and ν_3 modes of the $^2A_2$ and $^2B_1$ sates are mixture of the C_2–H stretching and C_3–H stretching motions. The phase of these motions are in consistent with that of the ground state. However, the main components of the ν_2 and ν_3 modes of the $^2A_2$ state change from those of the ground state. The main components of the ν_2 and ν_3 modes of $^2A_2$ are the C_3–H and C_2–H stretching motions, respectively. The coupling of the C_2–H and C_3–H stretching motions in the ν_2 and ν_3 modes of the $^2A_1$ and $^2B_2$ states becomes more weak. The ν_2 modes of the $^2A_1$ and $^2B_2$ states are assigned to the C_3–H and C_2–H stretching motions, respectively. The ν_3 modes of the $^2A_1$ and $^2B_2$ states are interpreted as the C_2–H and C_3–H stretching motions, respec-

TABLE IV. Vibrational frequencies (cm^{-1}).

State	ν_1	ν_2	ν_3	ν_4	ν_5	ν_6	ν_7	ν_8	ν_9
$^1A_1$	3914	3429	3405	1634	1537	1255	1150	1095	961
Obs.[a]	3400	3133	3100	1467	1384	1237	1144	1076	711
$^2A_2$	3824	3442	3426	1689	1581	1266	1166	1146	956
$^2B_1$	3768	3457	3431	1532	1517	1236	1118	1031	944
$^2A_1$	3856	3448	3384	1751	1394	1168	1135	873	539
$^2B_2$	3802	3423	2937	1645	1396	1214	1099	956	720

[a]Herzberg (Ref. 19).

TABLE V. Conventional potential energy distribution (%).

Component	ν_1	ν_2	ν_3	ν_4	ν_5	ν_6	ν_7	ν_8	ν_9
$^1A_1$ state									
ΔS_1	0.7	0.3	0.2	18.5	2.4	37.9	57.0	17.4	0.0
ΔS_2	0.0	0.9	0.0	14.8	19.3	18.4	6.1	0.0	0.0
ΔS_3	0.0	63.7	32.5	0.0	0.1	0.3	0.1	0.0	0.0
ΔS_4	0.0	32.1	63.3	0.1	0.0	0.4	0.0	0.1	0.0
ΔS_5	96.0	0.0	0.0	0.0	0.0	0.1	0.0	0.0	0.0
ΔS_6	2.4	1.9	0.7	44.5	11.0	7.1	1.8	40.7	52.4
ΔS_7	0.8	1.0	3.2	1.3	48.9	14.0	6.8	7.2	46.8
ΔS_8	0.1	0.0	0.0	19.6	0.0	11.9	21.9	6.8	0.0
ΔS_9	0.0	0.0	0.1	1.2	18.3	10.1	6.3	27.7	0.8
$^2A_2$ state									
ΔS_1	1.0	0.1	0.5	26.3	10.5	54.6	19.8	16.7	0.0
ΔS_2	0.0	0.6	0.1	0.1	9.5	13.9	8.7	24.8	0.1
ΔS_3	0.0	20.3	71.6	0.0	0.0	0.4	0.0	0.0	0.0
ΔS_4	0.0	78.0	18.7	0.4	0.0	0.3	0.0	0.1	0.0
ΔS_5	93.8	0.0	0.0	0.1	0.0	0.1	0.1	0.0	0.0
ΔS_6	3.8	0.9	2.7	22.9	40.8	7.9	23.5	35.1	50.2
ΔS_7	1.3	0.0	6.2	22.6	28.0	14.2	0.1	0.3	49.3
ΔS_8	0.1	0.0	0.0	12.9	9.1	3.0	0.1	22.8	0.0
ΔS_9	0.0	0.0	0.1	14.8	2.2	5.7	47.7	0.1	0.4
$^2B_1$ state									
ΔS_1	0.7	0.4	0.1	30.1	2.6	24.6	53.5	19.4	0.4
ΔS_2	0.0	0.8	0.1	17.7	22.9	1.5	7.5	2.6	0.3
ΔS_3	0.0	81.8	14.0	0.2	0.1	0.1	0.1	0.0	0.0
ΔS_4	0.0	13.4	83.6	0.4	0.0	0.0	0.0	0.2	0.0
ΔS_5	96.1	0.1	0.0	0.1	0.0	0.1	0.1	0.0	0.0
ΔS_6	2.3	1.9	0.3	8.7	37.2	6.1	21.8	26.3	50.7
ΔS_7	0.8	1.7	2.0	12.2	21.8	19.0	0.7	33.6	48.1
ΔS_8	0.1	0.1	0.0	5.9	12.5	23.6	9.0	7.6	0.0
ΔS_9	0.0	0.0	0.1	24.8	2.8	25.1	7.3	10.3	0.5
$^2A_1$ state									
ΔS_1	0.5	0.0	0.3	15.7	25.7	20.8	26.4	0.2	1.5
ΔS_2	0.0	1.5	0.2	43.3	30.3	2.6	0.8	0.0	4.4
ΔS_3	0.0	3.9	93.7	0.1	0.3	0.2	0.0	0.0	0.0
ΔS_4	0.0	94.6	4.1	0.6	0.7	0.0	0.0	0.0	0.0
ΔS_5	98.6	0.0	0.0	0.0	0.1	0.0	0.2	0.0	0.0
ΔS_6	0.7	0.1	0.6	18.5	0.0	2.3	23.5	45.2	42.0
ΔS_7	0.2	0.0	1.0	2.6	9.8	18.2	15.3	45.6	42.3
ΔS_8	0.1	0.0	0.1	19.1	16.5	41.3	0.5	0.3	6.7
ΔS_9	0.0	0.0	0.1	0.2	16.7	14.6	33.4	8.7	3.2
$^2B_2$ state									
ΔS_1	1.0	0.8	0.0	19.8	20.6	20.6	4.5	1.4	1.7
ΔS_2	0.0	0.2	0.0	0.6	1.1	6.3	9.9	8.5	3.3
ΔS_3	0.1	91.0	0.8	0.0	0.0	0.2	0.0	0.2	0.0
ΔS_4	0.0	0.4	94.0	1.8	0.9	0.3	0.0	0.0	0.6
ΔS_5	93.5	0.1	0.0	0.1	0.0	0.0	0.0	0.0	0.0
ΔS_6	4.0	3.2	0.3	23.9	48.0	20.6	65.6	0.6	35.5
ΔS_7	1.4	4.2	4.6	39.0	21.3	39.4	17.8	0.2	58.2
ΔS_8	0.1	0.0	0.1	7.6	8.0	10.5	2.0	3.3	0.4
ΔS_9	0.0	0.0	0.2	7.1	0.1	2.1	0.1	85.8	0.3

The definitions of the total symmetrical coordinates are as follows:
$\Delta S_1 = 1/\sqrt{2}(\Delta N\text{–}C_2 + \Delta N\text{–}C_5)$,
$\Delta S_2 = 1/\sqrt{2}(\Delta C_2\text{–}C_3 + \Delta C_4\text{–}C_5)$,
$\Delta S_3 = 1/\sqrt{2}(\Delta C_2\text{–}H + \Delta C_5\text{–}H)$,
$\Delta S_4 = 1/\sqrt{2}(\Delta C_3\text{–}H + \Delta C_4\text{–}H)$,
$\Delta S_5 = \Delta N\text{–}H$,
$\Delta S_6 = \Delta C_2\text{–}N\text{–}C_5$,
$\Delta S_7 = 1/\sqrt{2}(\Delta N\text{–}C_2\text{–}C_3 + \Delta N\text{–}C_5\text{–}C_4)$,
$\Delta S_8 = 1/\sqrt{2}(\Delta N\text{–}C_2\text{–}H + \Delta N\text{–}C_5\text{–}H)$ and
$\Delta S_9 = 1/\sqrt{2}(\Delta C_2\text{–}C_3\text{–}H + \Delta C_5\text{–}C_4\text{–}H)$.

TABLE VI. Classical half amplitude of the zero-point vibrational levels. Bond lengths are in angstroms, angles in degrees.

Component	ν_1	ν_2	ν_3	ν_4	ν_5	ν_6	ν_7	ν_8	ν_9
$^1A_1$ state									
$\Delta N-C_2$	−0.004	−0.003	0.002	−0.022	−0.004	0.021	0.022	0.013	0.002
ΔC_2-C_3	−0.000	−0.006	−0.001	0.023	−0.029	0.018	−0.012	−0.001	0.001
ΔC_2-H	0.002	0.062	−0.038	0.000	−0.002	0.003	0.001	−0.000	−0.001
ΔC_3-H	0.000	0.038	0.062	0.003	−0.000	0.003	0.000	−0.001	0.000
$\Delta N-H$	0.097	−0.002	0.001	−0.001	−0.002	0.002	0.001	0.001	0.001
ΔC_2-N-C_5	0.5	−0.4	0.2	1.8	−1.1	−0.4	−0.1	−1.0	−3.4
$\Delta N-C_2-C_3$	−0.2	0.2	−0.4	−0.1	1.5	0.5	−0.4	−0.4	2.6
$\Delta N-C_2-H$	0.2	−0.2	0.1	4.8	−0.6	−2.0	3.4	1.8	0.3
ΔC_2-C_3-H	0.0	0.1	−0.3	1.7	4.4	2.0	−2.2	3.3	−1.6
$^2A_2$ state									
$\Delta N-C_2$	−0.004	−0.001	−0.003	−0.017	−0.019	−0.023	0.012	0.012	0.000
ΔC_2-C_3	−0.000	−0.005	−0.002	0.000	0.028	−0.019	0.012	−0.027	0.005
ΔC_2-H	0.002	0.034	0.064	−0.001	0.001	−0.004	0.001	−0.000	−0.001
ΔC_3-H	0.000	0.064	−0.034	0.004	−0.001	−0.003	−0.000	−0.002	0.001
$\Delta N-H$	0.098	−0.002	−0.002	−0.002	−0.001	−0.002	0.002	0.000	0.002
ΔC_2-N-C_5	0.5	−0.2	−0.4	0.8	2.0	−0.5	−0.6	−1.0	−3.3
$\Delta N-C_2-C_3$	0.3	−0.1	−0.2	2.8	4.1	0.6	−0.1	−0.1	2.6
$\Delta N-C_2-H$	−0.2	0.0	0.5	0.8	−1.2	−1.5	0.2	3.7	0.0
ΔC_2-C_3-H	0.0	−0.1	0.3	3.6	−1.9	2.1	4.5	−0.3	−1.3
$^2B_1$ state									
$\Delta N-C_2$	−0.004	−0.003	0.001	−0.010	−0.014	0.017	−0.019	0.027	−0.012
ΔC_2-C_3	−0.000	−0.006	−0.002	−0.026	0.024	0.017	0.011	−0.015	0.010
ΔC_2-H	0.002	0.068	−0.024	−0.003	0.002	0.002	−0.001	0.000	−0.002
ΔC_3-H	0.000	0.024	0.069	−0.000	0.002	0.003	−0.002	−0.001	0.000
$\Delta N-H$	0.099	−0.003	0.001	−0.001	−0.001	0.002	−0.001	0.003	0.001
ΔC_2-N-C_5	0.5	−0.4	0.1	−0.8	2.0	−0.6	1.0	−2.3	−2.7
$\Delta N-C_2-C_3$	−0.2	0.3	−0.3	1.4	−0.6	0.6	−0.9	−0.0	2.5
$\Delta N-C_2-H$	0.3	−0.2	0.1	0.6	5.9	3.6	2.9	0.3	−1.0
ΔC_2-C_3-H	0.0	0.1	−0.3	4.6	0.8	−1.9	−0.5	1.8	−0.1
$^2A_1$ state									
$\Delta N-C_2$	−0.004	−0.000	−0.003	−0.020	−0.020	0.016	0.021	0.001	0.002
ΔC_2-C_3	−0.000	−0.007	−0.002	0.033	−0.022	−0.007	0.003	−0.001	−0.004
ΔC_2-H	0.001	0.014	0.072	0.002	−0.003	0.002	0.001	0.000	0.001
ΔC_3-H	0.001	0.071	−0.014	0.005	−0.004	−0.000	0.000	−0.001	−0.000
$\Delta N-H$	0.097	−0.002	−0.002	−0.001	−0.002	0.000	0.002	−0.001	−0.001
ΔC_2-N-C_5	0.5	−0.1	−0.4	2.0	−0.1	0.7	−1.7	3.1	1.2
$\Delta N-C_2-C_3$	−0.2	−0.0	0.5	−0.6	1.0	−1.3	1.1	−2.6	0.9
$\Delta N-C_2-H$	0.3	−0.1	−0.2	3.8	2.6	4.4	0.7	−0.5	−0.9
ΔC_2-C_3-H	0.0	−0.0	0.3	0.5	3.4	−3.3	4.7	2.9	0.7
$^2B_2$ state									
$\Delta N-C_2$	−0.004	−0.004	−0.001	−0.013	−0.028	0.020	0.012	0.002	−0.010
ΔC_2-C_3	−0.000	−0.004	0.001	−0.005	0.011	0.021	−0.035	0.012	0.027
ΔC_2-H	0.003	0.072	−0.005	−0.000	−0.001	0.004	−0.001	0.001	0.001
ΔC_3-H	0.000	0.005	0.078	0.010	−0.012	−0.006	0.002	0.001	−0.012
$\Delta N-H$	0.098	−0.004	−0.000	−0.002	−0.002	0.002	0.000	0.001	0.001
ΔC_2-N-C_5	0.5	−0.4	0.1	0.7	2.2	1.2	−2.5	−0.2	−2.3
$\Delta N-C_2-C_3$	−0.2	0.4	−0.4	0.9	−1.1	−1.3	1.1	0.1	2.4
$\Delta N-C_2-H$	0.3	−0.2	0.3	2.1	4.4	3.9	2.0	1.0	1.3
ΔC_2-C_3-H	0.0	0.2	−0.6	2.5	−0.4	−2.0	0.6	6.0	−1.6

tively. Tables V and VI reveal that the ν_9 mode of the $^2A_2$ state and the ν_8 mode of the $^2A_1$ state have the same character as the ν_9 mode of the ground state. The character of these modes are mixture of the C–N–C and N–C–C bending motions coupled out of phase. However, the PEDs of the ν_9 modes of the $^2B_1$ and $^2B_2$ states are almost same as that of the ground state, the classical half amplitude of these modes are different from that of the ground state. In these state, a coupling of the N–C and C–C stretching motions become large. The ν_4 and ν_5 modes of the $^2B_1$ state may be corresponded to the ν_5 and ν_4 modes of the ground state, respectively, since a good correspondence is found in the classical half amplitude of these modes. The ν_4 mode of the $^2A_1$ state may be also corresponded to the ν_4 mode of the ground state. However, we are not able to find any correspondence in the another modes between the ionic states and the ground state.

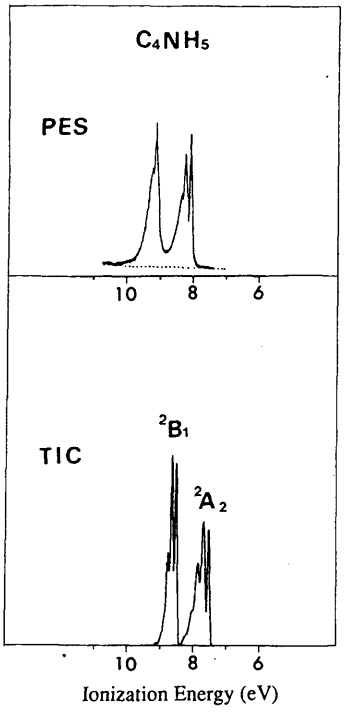

FIG. 2. The theoretical intensity curves of ionization of the $^2A_2$ and $^2B_1$ states with a halfwidth of 0.08 eV and the observed photoelectron spectrum by Turner *et al.* (Ref. 2). TIC: Theoretical intensity curve; PES: PE spectrum.

The theoretical intensity curve of the $^2A_2$ and $^2B_1$ states is shown in Fig. 2 by assuming a halfwidth of 0.08 eV for each transition band. It is compared with the observed PE spectrum by Turner *et al.*[2] The theoretical intensity curve imitates well the vibrational structure of the observed PE spectrum. In order to discuss more detailed vibrational structure of each band, we illustrate the theoretical intensity curve with a halfwidth of 0.02 eV in Figs. 3 and 4. The assignment of the vibrational structures of the $^2A_2$ and $^2B_1$ states are found in Tables VII and VIII, respectively.

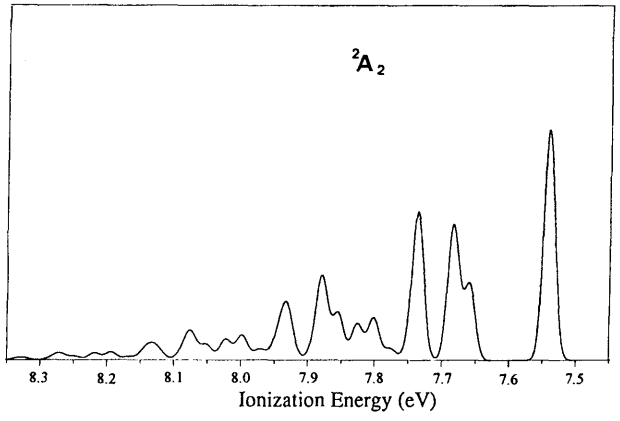

FIG. 3. The theoretical intensity curves of ionization of the $^2A_2$ state with a halfwidth of 0.02 eV.

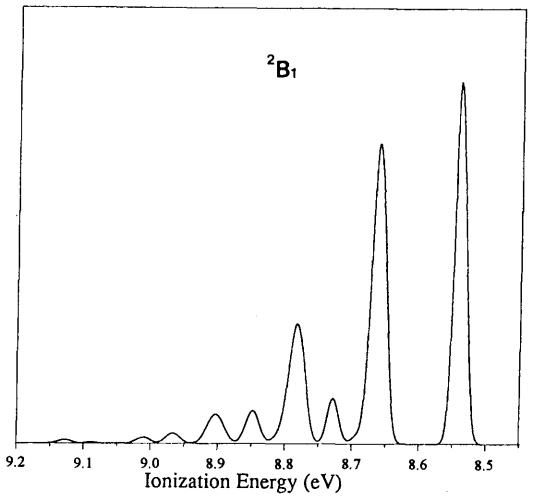

FIG. 4. The theoretical intensity curves of ionization of the $^2B_1$ state with a halfwidth of 0.02 eV.

Table VII shows the vibrational energy, intensity and assignment of each vibrational level of the $^2A_2$ state, where the vibrational level of which FCFs value are larger than 0.01 is listed. Intensity of each vibrational level is classify into a *S*, *M*, or *W* according to the magnitude of FCF. The present assignment is compared to the interpretation of the observed spectrum by Derrick *et al.*[3] We note that they reported by using the qualitative description of the vibrational modes according to Lord and Miller.[20] We rearrange their notation in Table VII according to Herzberg.[19] Comparing vibrational energies of the present calculation with those by Derrick *et al.* we overestimate from 8.1% to 15.3%. The present interpretation of the observed vibrational energies of 871 and 1742 cm^{-1} is in consistent with that by Derrick *et al.* The vibrational energies of 871 and 1742 cm^{-1} were assigned to the ν_9 and $2\nu_9$ transitions. The observed vibrational energy of 1065 cm^{-1} with strong intensity was assigned to only the ν_8 mode by them. The present calculation shows that the ν_7 mode also contribute to intensity, and that the FCF of the excitation of the ν_7 mode is almost the same value as that of the ν_8 mode. We obtained from calculation nearly equal values of frequencies of the ν_7 (1146 cm^{-1}) and ν_8 (1166 cm^{-1}) modes, therefore, we could not separated each band in the theoretical intensity curve. Derrick *et al.* assigned the observed vibrational energies of 1936, 2129, and 2460 cm^{-1} to the $\nu_8+\nu_9$, $2\nu_8$, and $\nu_5+\nu_8$ transitions, respectively. We find that the intensity of the $\nu_7+\nu_9$, $\nu_7+\nu_8$, and $\nu_5+\nu_7$ transitions are also strong as those transitions. Derrick *et al.* interpreted the observed frequencies of 1371 and 1468 cm^{-1} as the ν_5 and ν_4 modes, respectively. These interpretation should be supported by the present calculation. However, they reported that the intensity of the ν_5 and ν_4 bands were same. The present calculation of FCFs of ν_5 and ν_4 give strong and weak intensity, respectively. They reported weak bands of the frequencies of 2541 and 2839 cm^{-1} which were interpreted as $\nu_4+\nu_8$ and $\nu_4+\nu_5$, respectively. The value of FCFs of these transitions were smaller than 0.01. Therefore, we could not find any peak in the theoretical

TABLE VII. Assignment of the vibrational structure of the $^2A_2$ state. IE: Ionization energy. Intensity of the present calculation is classified into *S*, *M*, or *W*, according to magnitude of FCF as followings: *S*:0.21>FCF >0.13, *M*:0.08>FCF>0.03 or *W*:0.03>FCF>0.01. Derrick *et al.* have used the qualitative description of the vibrational modes according to Loard and Miller. Their assignment of the modes are rearranged by according to Herzberg.

Present calculation					Derrick *et al.*[a]		
IE	Vibrational energy (cm^{-1})	Intensity	Assignment		Vibrational energy (cm^{-1})	Intensity	Assignment
7.54	0	*S*	0		0	*VS*	0
7.66	956	*M*	ν_9		871	*M*	ν_9
7.68	1146,1166	*S*	ν_7,	ν_8	1065	*S*	ν_8
7.74	1581	*S*	ν_5		1371	*M*	ν_5
7.75	1689	*W*	ν_4		1468	*M*	ν_4
7.78	1912	*W*	$2\nu_9$		1742	*W*	$2\nu_9$
7.80	2102,2122	*M*	$\nu_7+\nu_9$,	$\nu_8+\nu_9$	1936	*MW*	$\nu_8+\nu_9$
7.83	2292,2312	*W*	$2\nu_8$,	$\nu_7+\nu_8$	2129	*MW*	$2\nu_8$
7.85	2537	*M*	$\nu_5+\nu_9$				
7.88	2727,2747	*M*	$\nu_5+\nu_7$,	$\nu_5+\nu_8$	2460	*W*	$\nu_5+\nu_8$
7.93	3162	*M*	$2\nu_5$				
8.00	3683,3703	*W*	$\nu_5+\nu_7+\nu_9$,	$\nu_5+\nu_8+\nu_9$			
8.05	4118	*W*	$2\nu_5+\nu_9$				
8.08	4308,4328	*W*	$2\nu_5+\nu_7$,	$2\nu_5+\nu_8$			
8.13	4743	*W*	$3\nu_5$				

[a]Reference 3.

intensity curve correspond to these transitions. The band of the $\nu_5+\nu_9$ transition is found in the present result. Derrick *et al.* should miss this band which could be observed between 2129 and 2460 cm^{-1}.

We are able to connect the contribution of each mode to intensity with the change in geometrical parameters by ionization. Table I reveals that the $N-C_2$ length becomes short and the C_2-C_3 length becomes long. Table VI shows that a magnitude in the change of the C_2-C_3 length is larger than that of the classical half amplitude of the zero-point vibrational level of each mode. The character of the ν_5 is mixture of the $N-C_2$ and C_2-C_3 stretching motions coupled with out phase mode. This phase is in consistent with the phase of the change in $N-C_2$ and C_2-C_3 length. The ν_8 mode is also couple the $N-C_2$ and C_2-C_3 stretching motions with out phase mode. Therefore, the higher vibrational excitation including the ν_5 and ν_8 modes mainly contribute intensity.

Table VIII shows the assignment of the vibrational structure of the $^2B_1$ state. The first peak of the theoretical intensity curve is the zero–zero transition state. Derrick *et al.* interpreted the observed second peak with the vibrational energy of 871 cm^{-1} as the ν_9 mode only. The present calculation suggests that the ν_8 mode also contributes to the second peak. The intensity of the transition of the ν_8 mode is strong as that of the ν_9 mode. The present calculation also shows that the ν_5 mode contributes to intensity.

Table I shows that the C_2-N-C_5 angle of $^2B_1$ becomes wide by 4.4°. A magnitude of the change is larger than that of

TABLE VIII. Assignment of the vibrational structure of the $^2B_1$ state. Intensity of the present calculation is classified into *S*, *M* or *W* according to magnitude of FCF as followings: *S*:0.33>FCF>0.13, *M*:0.08>FCF >0.03 or *W*:0.03>FCF>0.01.

Present calculation				Derrick *et al.*[a]		
IE	Vibrational energy (cm^{-1})	Intensity	Assignment	Vibrational energy (cm^{-1})	Intensity	Assignment
8.54	0	*S*		0	*VS*	0
8.66	944	*S*	ν_9	871	*S*	ν_9
8.67	1031	*S*	ν_8			
8.73	1517	*M*	ν_5			
8.77	1888	*M*	$2\nu_9$			
8.78	1975	*M*	$\nu_8+\nu_9$			
8.80	2062	*W*	$2\nu_8$			
8.44	2461	*W*	$\nu_5+\nu_9$			
8.86	2548	*W*	$\nu_5+\nu_8$			
8.90	2919	*W*	$\nu_8+2\nu_9$			
8.91	3006	*W*	$2\nu_8+\nu_9$			

[a]Reference 3.

the classical half amplitude of the zero-point vibrational level of each mode. The C_2–N–C_5 bending motion have an amplitude in the ν_5, ν_8, and ν_9 modes. Therefore, these modes should contribute to intensity.

For the $^2A_1$ and $^2B_2$ states, we could not obtain reasonable theoretical intensity curves compared with the observed spectra. Large geometrical changes are found in the N–C–C and C_2–C_3–H bond angles of the $^2A_1$ state and the N–C_2–H and C_2–C_3–H bond angles of the $^2B_2$ state. A magnitude of these change is considerably large compared to that of the classical half amplitude of the zero-point vibrational level of each mode. Therefore, higher vibrational excitations of the bending modes should contribute to intensity.

IV. CONCLUSION

The molecular equilibrium structures and vibrational frequencies were calculated for the ground and lower four ionic states. By the use of the FCFs, we obtained the transition intensity curve of the $^2A_2$ and $^2B_1$ states. The theoretical intensity curves were in good agreement with the the observed PE spectra.

The vibrational structure of the spectrum of $^2A_2$ were interpreted using the ν_4, ν_5, ν_8, and ν_9 modes by Derrick *et al.* The present calculation shows that the ν_7 mode also contributes to spectrum. The frequency and intensity of the ν_7 mode are nearly equal to those of the ν_8 mode. A contribution of the ν_4 mode to intensity is negligibly small. The character of the ν_9 mode is out of phase mode of the C–N–C bending and N–C–C bending motions, which is the same character as the ν_9 mode of the ground state. However, we could not connect the character of the ν_4, ν_5, ν_7, and ν_8 modes with that of the ground state. We could not also interpret clearly of these mode, because we find complicated mixture of the N–C stretching, C–C stretching, bending of ring, N–C–H bending and C–C–H bending motions in these modes.

Derrick *et al.* assigned the second peak of the vibrational structure of the $^2B_2$ state by using the ν_9 mode only. The present calculation shows that the ν_8 mode also contributes to the second peak which intensity is equal to that of the ν_9 transition. The character of the ν_9 mode is the same as that of the ground state.

We could not reasonable theoretical intensity curves of the $^2A_1$ and $^2B_2$ states because of a large geometrical change in the C_2–C_3–H bond angles by ionization.

ACKNOWLEDGMENT

Computation was carried out on HITAC M-680H systems at the Center for Information Processing Education of Hokkaido University.

[1] A. D. Baker, D. Betteride, N. R. Kemp, and R. E. Kirby, Anal. Chem. **42**, 1064 (1970).
[2] D. W. Turner, A. D. Baker, C. Baker, and C. R. Brundel, *Molecular Photoelectron Spectroscopy* (Wiley-Interscience, London, 1970).
[3] P. J. Derrick, L. Åsbrink, O. Edqvist, and E. Lindholm, Spectrochim. Acta A **27**, 2525 (1971).
[4] J. A. Sell and A. Kuppermann, Chem. Phys. Lett. **15**, 355 (1979).
[5] T. Munakata, K. Kuchitu, and Y. Harada, J. Electron Spectrosc. Relat. Phenom. **20**, 235 (1980).
[6] K. Kimura, S. Katsumata, Y. Achiba, T. Yamazaki, and S. Iwata, *Handbook of HeI Photoelectron Spectra of Fundamental Organic Molecules* (Halsted, New York, 1981).
[7] L. Klasinc, A. Sabljic, G. Kluge, J. Rieger, and M. Scholz, J. Chem. Soc., Perkin Trans. 2 539 (1982)
[8] W. von Niessen, L. S. Cederbaum, and G. H. F. Diercksen, J. Am. Chem. Soc. **98**, 2066 (1976).
[9] G. Dealti, P. Decleva, and A. Lisini, Chem. Phys. **90**, 231 (1984).
[10] H. Nakatsuji, O. Kitao, and T. Yonezawa, J. Chem. Phys. **83**, 723 (1985).
[11] F. R. Cordell and J. E. Boggs, J. Mol. Struct. **85**, 163 (1981).
[12] H. Tatewaki and S. Huzinaga, J. Comput. Chem. **1**, 205 (1980).
[13] A. D. Mclean and B. Liu, J. Chem. Phys. **58**, 1066 (1973).
[14] T. Shoda, T. Noro, T. Nomura, and K. Ohno, Intern. J. Quantum Chem. **30**, 289 (1986).
[15] K. Takeshita, J. Chem. Phys. **86**, 329 (1987).
[16] K. Takeshita and F. Sasaki, 1981 Library program at the Hokkaido University Computing Center (in Japanese). GRAMOL included the Program JAMOL3 of the RHF calculation written by H. Kashiwagi, T. Takada, E. Miyoshi, and S. Obara for the Library program at the Hokkaido University Computing Center 1977 (in Japanese).
[17] A. Murakami, H. Iwaki, H. Terashima, T. Shoda, T, Kawaguchi and T. Noro, 1986 Library program at the Hokkaido University Computing Center (in Japanese).
[18] L. Nygaard, J. T. Nielsen, J. Kirchheiner, G. Maltesen, J. Rastrup-Andersen, and G. O. Soreensen, J. Mol. Struct. **3**, 491 (1969).
[19] G. Herzberg, *Molecular Spectra and Molecular Structure*, Part III (Van Nostrand, New York, 1966).
[20] R. C. Loard, Jr., and F. A. Miller, J. Chem. Phys. **10**, 328 (1942).